J|A|C|S
ARTICLES

Light-Driven Reversible Handedness Inversion in Self-Organized Helical Superstructures

Manoj Mathews,[†] Rafael S. Zola,[†] Shawn Hurley,[†] Deng-Ke Yang,[†]
Timothy J. White,[‡] Timothy J. Bunning,[‡] and Quan Li*,[†]

Liquid Crystal Institute and Chemical Physics Interdisciplinary Program, Kent State University, Kent, Ohio 44242, United States, and Materials and Manufacturing Directorate, Air Force Research Laboratory, WPAFB, Ohio 45433, United States

Received September 17, 2010; E-mail: qli1@kent.edu

Abstract: We report here a fast-photon-mode reversible handedness inversion of a self-organized helical superstructure (i.e., a cholesteric liquid crystal phase) using photoisomerizable chiral cyclic dopants. The two light-driven cyclic azobenzenophanes with axial chirality show photochemically reversible trans to cis isomerization in solution without undergoing thermal or photoinduced racemization. As chiral inducing agents, they exhibit good solubility, high helical twisting power, and a large change in helical twisting power due to photoisomerization in three commercially available, structurally different achiral liquid crystal hosts. Therefore, we were able to reversibly tune the reflection colors from blue to near-IR by light irradiation from the induced helical superstructure. More interestingly, the different switching states of the two chiral cyclic dopants were found to be able to induce a helical superstructure of opposite handedness. In order to unambiguously determine the helical switching, we employed a new method that allowed us to directly determine the handedness of the long-pitched self-organized cholesteric phase.

Introduction

Self-organization of chiral molecules into reversibly tunable helical systems with amplified chiral properties is a rapidly growing scientific area of contemporary interest.[1] A cholesteric liquid crystal (CLC) phase is one such self-organized system. In the cholesteric or chiral nematic (N*) phase, molecules self-organize into a helical arrangement characterized by both handedness and helical pitch, P.[2] Handedness describes the direction in which the molecular orientation (called the director) rotates along the helical axis, and P is defined as the distance over which the director rotates by a full 360°. When light propagates through the CLC film, it selectively reflects light of a specific wavelength band ($\Delta\lambda$) that matches with the pitch of the helix according to eq 1:

$$\Delta\lambda = \Delta n P \cos\theta \tag{1}$$

where Δn is the effective refractive index and θ is the angle between the incident light and the helical axis (Figure 1). A number of stimuli, including temperature,[3] light,[4,5] electric field,[6] mechanical stress,[7] and chiral-dopant concentration,[8] have been employed to tune the wavelength of the reflected light by changing the helical pitch. This constitutes the basis for the application of cholesteric materials in reflection displays,[9] color

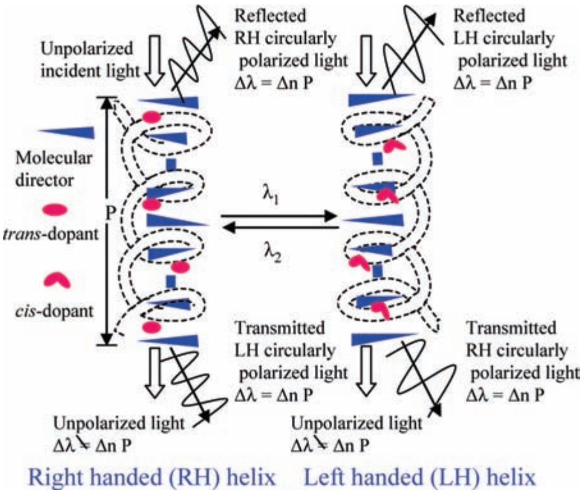

Figure 1. Schematic representation of light-controlled reversible switching of the handedness and the reflection colors of an induced helical superstructure by photoisomerization of a chiral azo dopant.

[†] Kent State University.

[‡] Air Force Research Laboratory.

(1) (a) *Chirality at the Nanoscale: Nanoparticles, Surfaces, Materials, and More*; Amabilino, D. B., Ed.; Wiley-VCH: Weinheim, Germany, 2009. (b) Pijper, D.; Feringa, B. L. *Soft Matter* **2008**, *4*, 1349–1372. (c) Maeda, K.; Mochizuki, H.; Watanabe, M.; Yashima, E. *J. Am. Chem. Soc.* **2006**, *128*, 7639–7650. (d) Green, M. M.; Zanella, S.; Gu, H.; Sato, T.; Gottarelli, G.; Jha, S. K.; Spada, G. P.; Schoevaars, A. M.; Feringa, B. L.; Teramoto, A. *J. Am. Chem. Soc.* **1998**, *120*, 9810–9817.

(2) (a) *The Physics of Liquid Crystals*; de Gennes, P. G., Prost, J., Eds.; Oxford University Press: Oxford, U.K., 1993. (b) Collings, P. J.; Hird, M. *Introduction to Liquid Crystals: Chemistry and Physics*; Taylor & Francis: London, 1997. (c) *Chirality in Liquid Crystals*; Kitzerov, H.-S., Bahr, C., Eds.; Springer: New York, 2001.

(3) (a) Gleeson, H. F. In *Handbook of Liquid Crystals*; Demus, D., Goodby, J., Gray, G. W., Spiess, H. W., Vill, V., Eds.; Wiley-VCH: Weinheim, Germany, 1998; Vol. 1, Chapter 9, p 823. (b) Zhang, F.; Yang, D.-K. *Liq. Cryst.* **2002**, *29*, 1497–1501.

reflectors and filters,[10] tunable lasers,[11] molecular sensors,[12] and other biomedical applications.[13] The utility of thermal, electrical, and light-induced color switching and tuning has been reviewed by White et al.[14]

The circularly polarized nature of the reflected light is another remarkable property associated with CLCs. When unpolarized light impinges on the CLC material, circularly polarized light with the same handedness as the helix is reflected.[2] Circularly polarized light with the opposite handedness is transmitted through the sample. Outside the reflection band, incident light is transmitted regardless of its polarization state, as shown in Figure 1. Selective preparation of right- or left-handed CLC films is achieved from intrinsically chiral LC molecules or LC mixtures containing chiral dopants. Enantiomers of a chiral mesogen or chiral dopant are used to obtain an equal but opposite twist in the cholesteric phase.[8] On the other hand, switching of the cholesteric helicity in response to external stimuli such as temperature, light, or electric field can significantly improve and/or widen the area of potential applications of CLC materials.[10]

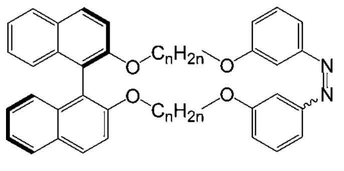

1 n = 3; **2** n = 5

Figure 2. Molecular structure of the axially chiral azobenzenophanes (*R*)-**1** and (*R*)-**2** used as switch molecules in the present study.

In comparison with the large body of literature describing the tunability of the cholesteric pitch to obtain red, green, and blue reflection colors,[3−10] a reversible switching of the cholesteric handedness by external stimuli such as temperature and light remains a challenging task.[15−19] Temperature-dependent helix inversion can be attributed to either a change in molecular conformations[15] or a shift in the equilibrium between opposite chiralities of multiple chiral centers.[16] For practical applications, these systems cause some serious drawbacks because of the requirement of above-ambient-temperature conditions. Therefore, a light-controlled twist inversion in CLCs is more attractive. To date, CLC mixtures having phototunable chiral dopants have been studied as a step toward achieving this goal, but only a few demonstrations of helicity switching have been published.[17−19] Such switching requires that the photoresponsive molecule employed as a dopant either reverses its intrinsic chirality (e.g., sterically overcrowded alkenes)[17] or forms different switching states capable of inducing the opposite cholesteric helix (e.g., trans−cis isomerization in some chiral azobenzenes)[18,19] under light irradiation. In these reports, either a relatively slow thermal isomerization process of the dopant drives the reversible switching to the initial state,[16,18] the helical handedness inversion is limited to a particular nematic liquid crystal (NLC) host,[17] or the helical twisting power (HTP) of the dopant is low.[19]

Here we report photoinvertible CLCs based on the helical inversion of chiral cyclic azobenzenophanes (*R*)-**1** and (*R*)-**2** (Figure 2) in three structurally different, commercially available NLC hosts. It is noteworthy that the compounds used here not only show higher HTP than a structurally similar known chiral dopant[20] and reversible control of the selective reflection colors from blue to near-IR (NIR) but also reveal the unique capability to induce a reversible helical twist inversion in the cholesteric phase by light irradiation.

Results and Discussion

Materials Design and Synthesis. Compounds (*R*)-**1** and (*R*)-**2** consist of an axially chiral binaphthyl moiety [(*R*)-(+)-1,1′-bis(2-naphthol)] bonded to the meta positions of a photoresponsive azobenzene through methylene linkages. There are three methylene linking units in (*R*)-**1**, while (*R*)-**2** has five linking methylene groups, making the latter compound conformationally more flexible. Both compounds were successfully synthesized by reduction of their corresponding dinitro compounds using

---

(4) (a) Eelkema, R.; Feringa, B. L. *Org. Biomol. Chem.* **2006**, *4*, 3729–3745. (b) Yoshioka, T.; Ogata, T.; Nonaka, T.; Moritsugu, M.; Kim, S. N.; Kurihara, S. *Adv. Mater.* **2005**, *17*, 1226–1229. (c) Mallia, V. A.; Tamaoki, N. *Chem. Soc. Rev.* **2004**, *33*, 76–84. (d) Ichimura, K. *Chem. Rev.* **2000**, *100*, 1847–1873.

(5) (a) Ma, J.; Li, Y.; White, T. J.; Urbas, A.; Li, Q. *Chem. Commun* **2010**, *46*, 3463–3465. (b) White, T. J.; Bricker, R. L.; Natarajan, L. V.; Tabiryan, N. V.; Li, Q.; Bunning, T. J. *Adv. Funct. Mater.* **2009**, *19*, 3484–3488. (c) Li, Q.; Green, L.; Venkataraman, N.; Shiyanovskaya, I.; Khan, A.; Urbas, A.; Doane, J. W. *J. Am. Chem. Soc.* **2007**, *129*, 12908–12909.

(6) (a) Bobrovsky, A.; Shibaev, V. *J. Mater. Chem.* **2009**, *19*, 366–372. (b) Chen, J.; Morris, S. M.; Wilkinson, T. D.; Coles, H. J. *Appl. Phys. Lett.* **2007**, *91*, 121118. (c) Lu, S.-Y.; Chen, L.-C. *Appl. Phys. Lett.* **2007**, *91*, 131119.

(7) (a) Finkelmann, H.; Kim, S. T.; Munoz, A.; Palffy-Muhoray, P.; Taheri, B. *Adv. Mater.* **2001**, *13*, 1069–1072. (b) Schmidtke, J.; Kniesel, S.; Finkelmann, H. *Macromolecules* **2005**, *38*, 1357–1363.

(8) Mathews, M.; Tamaoki, N. *J. Am. Chem. Soc.* **2008**, *130*, 11409–11416.

(9) (a) *Reflective Liquid Crystal Displays*; Wu, S.-T., Yang, D.-K., Eds.; Wiley: Chichester, U.K., 2001. (b) Yang, D.-K.; West, J. L.; Chien, L.-C.; Doane, J. W. *J. Appl. Phys.* **1994**, *76*, 1331–1333. (c) Tamaoki, N. *Adv. Mater.* **2001**, *13*, 1135–1147.

(10) (a) Ha, N. A.; Ohtsuka, Y.; Jeong, S. M.; Nishimura, S.; Suzaki, G.; Takanishi, Y.; Ishikawa, K.; Takezoe, H. *Nat. Mater.* **2008**, *7*, 43–47. (b) Mitov, M.; Dessaud, N. *Nat. Mater.* **2006**, *5*, 361–364. (c) Lub, J.; van de Witte, P.; Doornkamp, C.; Vogels, J. P. A.; Wegh, R. T. *Adv. Mater.* **2003**, *15*, 1420–1425. (d) Hochbaum, A.; Jiang, Y.; Li, L.; Vartak, S.; Faris, S. *SID Digest* **1999**, *30*, 1063–1065.

(11) (a) Kopp, V. I.; Fan, B.; Vithana, H. K. M.; Genack, A. Z. *Opt. Lett.* **1998**, *23*, 1707–1709. (b) Cao, W.; Munoz, A.; Palffy-Muhoray, P.; Taheri, B. *Nat. Mater.* **2002**, *1*, 111–113. (c) Furumi, S.; Tamaoki, N. *Adv. Mater.* **2010**, *22*, 886–891.

(12) Raynes, P.; Cowling, S. J.; Goodby, J. W. *Anal. Methods* **2009**, *1*, 88–92.

(13) (a) *Liquid Crystals: Frontiers in Biomedical Applications*; Woltman, S. J., Jay, G. D., Crawford, G. P., Eds.; World Scientific: Singapore, 2007. (b) Stewart, G. T. *Liq. Cryst.* **2003**, *30*, 541–557. (c) Hoogboom, J.; Clerx, J.; Otten, M. B. J.; Rowan, A. E.; Rasing, T.; Nolte, R. J. M. *Chem. Commun.* **2003**, 2856–2857. (d) Woltman, S. J.; Jay, G. D.; Crawford, G. P. *Nat. Mater.* **2007**, *6*, 929–938.

(14) White, J. T.; McConney, M. E.; Bunning, T. J. *J. Mater. Chem.* **2010**, *20*, 9832–9847.

(15) (a) Slaney, A. J.; Nishiyama, I.; Styring, P.; Goodby, J. W. *J. Mater. Chem.* **1992**, *2*, 805–810. (b) Styring, P.; Vuijk, J. D.; Slaney, A. J.; Goodby, J. W. *J. Mater. Chem.* **1993**, *3*, 399–405.

(16) (a) Stegemeyer, H.; Siemensmeyer, K.; Sucrow, W.; Appel, L. *Z. Naturforsch., A: Phys. Sci.* **1989**, *44*, 1127–1130. (b) Dierking, I.; Giesselmann, F.; Zugenmaier, P.; Kuczynski, W.; Lagerwall, S. T.; Stebler, B. *Liq. Cryst.* **1993**, *13*, 45–55. (c) Dierking, I.; Giesselmann, F.; Zugenmaier, P.; Mohr, K.; Zaschke, H.; Kuczynski, W. *Liq. Cryst.* **1995**, *18*, 443–449.

(17) (a) Feringa, B. L.; Huck, N. P. M.; van Doren, H. A. *J. Am. Chem. Soc.* **1995**, *117*, 9929–9930. (b) van Delden, R. A.; Koumura, N.; Harada, N.; Feringa, B. L. *Proc. Natl. Acad. Sci. U.S.A.* **2002**, *99*, 4945–4949. (c) Eelkema, R.; Pollard, M. M.; Katsonis, N.; Vicario, J.; Broer, D. J.; Feringa, B. L. *J. Am. Chem. Soc.* **2006**, *128*, 14397–14407.

(18) (a) van Delden, R. A.; Mecca, T.; Rosini, C.; Feringa, B. L. *Chem.—Eur. J.* **2004**, *10*, 61–70. (b) Pieraccini, S.; Gottarelli, G.; Labruto, R.; Masiero, S.; Pandolini, O. S.; Spada, G. P. *Chem.—Eur. J.* **2004**, *10*, 5632–5639.

(19) Mathews, M.; Tamaoki, N. *Chem. Commun.* **2009**, 3609–3611.

(20) Kawamoto, M.; Aoki, T.; Wada, T. *Chem. Commun.* **2007**, 930–932.

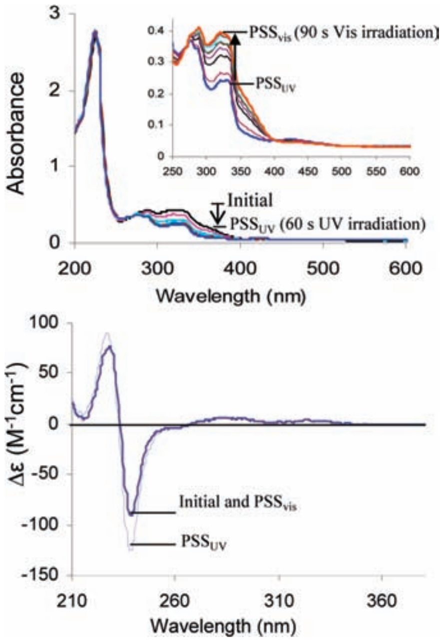

Figure 3. (top) Changes in the absorption spectra of (*R*)-**2** in acetonitrile (20 μM) upon irradiation with UV (365 nm) and visible (440 nm, inset) light at room temperature. (bottom) CD spectra of *trans*-(*R*)-**2** (black line) and the photostationary states (PSSs) resulting from irradiation at 365 nm (blue line) and 440 nm (red line) in acetonitrile solvent. It should be noted that the initial spectra (black lines) coincide exactly with the PSS_{vis} spectra (red lines).

$LiAlH_4$ under dilute conditions (Figure S1 in the Supporting Information). The crude products obtained were purified by column chromatography on silica gel. Their structures were identified by ^1H and ^{13}C NMR spectroscopy, high-resolution mass spectrometry (HRMS), and elemental analysis.

Data for (*R*)-1. ^1H NMR ($CDCl_3$): δ 7.80−7.76 (m, 4H, Ar), 7.54−7.25 (m, 14H, Ar), 6.90 (d, 2H, J = 8.0 Hz, Ar), 4.41−3.50 (m, 8H), 1.99−1.60 (m, 4H). ^{13}C NMR ($CDCl_3$): δ 159.5, 154.7, 153.5, 133.9, 129.8, 129.6, 129.3, 128.0, 126.2, 125.1, 124.0, 121.4, 120.3, 117.2, 115.2, 106.4, 66.6, 63.8, 29.4. HRMS *m*/*z*: calcd for $C_{38}H_{33}N_2O_4$ (M + H), 581.2440; found, 581.2457. Anal. Calcd for $C_{38}H_{33}N_2O_4$: C, 78.60; H, 5.55; N, 4.82. Found: C, 78.57; H, 5.60; N, 4.75.

Data for (*R*)-2. ^1H NMR ($CDCl_3$): δ 7.89−7.75 (m, 4H, Ar), 7.61−7.17 (m, 14H, Ar), 7.03 (d, 2H, J = 8.0 Hz, Ar), 4.02−3.80 (m, 8H), 1.60−1.17 (m, 12H). ^{13}C NMR ($CDCl_3$): δ 159.6, 154.7, 153.7, 134.2, 129.9, 129.5, 129.4, 127.9, 126.1, 125.5, 123.6, 121.1, 119.5, 116.7, 115.3, 107.7, 70.2, 68.0, 28.7, 27.5, 21.8. HRMS *m*/*z*: calcd for $C_{42}H_{41}N_2O_4$ (M + H), 637.3066; found, 637.3093.

Trans−Cis Isomerization and Chiroptical Properties. The absorption spectra of the trans isomer of (*R*)-**2** (Figure 3 top) show two distinct regions (one band below 250 nm and the other between 270−390 nm) that are characteristic of molecules having both naphthalene and azobenzene chromophores in their structures.[17,19,21] The absorption band below 250 nm mainly corresponds to the long-axis polarization (^1B transition) of the naphthalene chromophore. The band at 270−390 nm originates from $\pi \rightarrow \pi^*$ transitions of the azo chromophore and the short-axis polarizations (^1L_b and ^1L_a) of the naphthalene moiety. Similarly, the CD spectra show two distinct regions (Figure 3 bottom). Only weak Cotton bands due to azobenzene excitations are seen at 300−400 nm. An intense negative exciton couplet at 225 nm due to the long-axis-polarized transition of the naphthalene units reflects the absolute *R* configuration of the binaphthyl moiety in the molecule.[21] Compound (*R*)-**1** showed similar UV−vis and CD spectra (Figure S2 in the Supporting Information).

With the aim of studying the photoisomerization of the target compounds, a solution of (*R*)-**1** and (*R*)-**2** in acetonitrile was sequentially irradiated with UV light (λ_{max} = 365 nm, 6.0 mW/cm^2) and visible light (λ_{max} = 440 nm, 2.0 mW/cm^2). As expected, UV light induced trans−cis isomerization, as evidenced by the gradual decrease in the $\pi \rightarrow \pi^*$ transition bands in the absorption spectra with a concomitant small increase in the $n \rightarrow \pi^*$ band around 440 nm. A photostationary state (PSS) was reached within 60 s, and additional irradiation did not induce further changes in absorption. The top panel of Figure 3 shows the absorption spectral change in (*R*)-**2** upon trans−cis photoisomerization. Upon visible-light irradiation, reverse absorption spectral changes occurred, and a PSS_{vis} state was attained in 90 s.

The effect of photoisomerizations on the chirality of these compounds was studied by CD spectroscopy. UV irradiation did not switch the overall *R* chiral configuration of the compounds. However, the influence of trans−cis isomerization on the chiroptical properties of these compounds was clearly evident from the change in the intensity of the CD bands (Figure 3 bottom). The exciton couplet around 225 nm gradually increased upon UV irradiation, indicating a change in the dihedral angle of the binaphthyl moiety.[22] However, with UV irradiation, there was only a small decrease in the intensity of the $\pi \rightarrow \pi^*$ transitions of the trans isomer, and no concomitant increase in the $n \rightarrow \pi^*$ transition band due to the cis isomer was seen in the CD spectra. Upon irradiation with 440 nm light, fast reverse CD spectral changes occurred.

Photomodulation of Cholesteric Pitch and Reflection Colors. When a chiral dopant is dissolved in a host NLC, the induced cholesteric pitch *P* is correlated with the weight concentration C_w of the dopant (weight percentage of dopant in the host NLC) and its enantiomeric purity *r* according to eq 2:

$$P^{-1} = \beta C_w r \qquad (2)$$

in which the proportionality constant β is the helical twisting power.[4a] We determined the HTPs of (*R*)-**1** and (*R*)-**2** in three structurally different, commercially available NLCs, namely, E7 (a common eutectic cyanobiphenyl mixture), K15 (4-cyano-4′-pentylbiphenyl), and ZLI-1132 (a eutectic cyclohexane-based mixture).[23] Small amounts of (*R*)-**1** or (*R*)-**2** chiral guest molecules doped in the NLC induced a N* phase, which was evidenced as a fingerprint (long pitch) or an Granjean (short pitch) texture under a polarized optical microscope. The induced helical pitch and its phototunability were measured using Cano's wedge method,[24] and the corresponding change in the HTP value was calculated on

---

[21] Takaishi, K.; Kawamoto, M.; Tsubaki, K.; Wada, T. *J. Org. Chem.* **2009**, *74*, 5723–5728.

[22] Rosini, C.; Superchi, S.; Peerlings, H. W. I.; Meijer, E. W. *Eur. J. Org. Chem.* **2000**, 61–71.

[23] (a) E7 (T_{NI} = 60.5 °C): eutectic mixture of nematic cyanobiphenyls. (b) ZLI-1132 (T_{NI} = 72.3 °C): mixture of 4-(4-alkylcyclohexyl)benzonitrile and 4-(4-alkylcyclohexyl)-4′-cyanobiphenyl derivatives. (c) K15 (T_{NI} = 35.0 °C): 4-cyano-4′-pentylbiphenyl.

[24] *Textures of Liquid Crystals*; Dierking, I., Ed.; Wiley-VCH: Weinheim, Germany, 2003.

Table 1. Helical Twisting Powers (β) of Dopants in Different NLC Hosts As Determined by Cano's Wedge Method and the Observed Change in Values by Irradiation (Positive and Negative Values Represent Right- and Left-Handed Helical Twists, Respectively)

		β (wt%) μm^{-1}			
dopant	host NLC	initial	PSS$_{UV}$	PSS$_{vis}$	$\Delta\beta/\beta$ (%)[a]
(*R*)-**1**	E7	+40	+7	+30	83
	K15	+50	−10	+43	120
	ZLI-1132	+8	−26	+6	425
(*R*)-**2**	E7	+32	−10	+26	131
	K15	+12	−18	+8	250
	ZLI-1132	+32	−16	+24	150

[a] Percent change in β observed in going from the initial state to PSS$_{UV}$.

the basis of the above-mentioned equation. The results are summarized in Table 1.

Dopant (*R*)-**1** in its trans form shows a high HTP in E7 and K15, while the corresponding value in ZLI-1132 was found to be low. Its analogue (*R*)-**2** exhibits a lower HTP in E7 and K15 LC hosts than does (*R*)-**1**. On the contrary, the HTP of (*R*)-**2** in ZLI-1132 was found to be higher than that obtained for its lower homologue compound (*R*)-**1**. In comparison with its ortho-substituted analogue, the meta-substituted chiral dopant (*R*)-**1** exhibited a higher HTP and a larger change in HTP, which might result from the intrinsic nature of its molecular structure and having a more dramatic geometrical change upon photoisomerization. Using a different LC host results in different intermolecular association between the dopant and the host. These results clearly reveal the subtle dependence of HTP on the molecular structures of both the dopant and the NLC host. The helical sense of the induced N* phase was determined by either the contact or the reflection method.[24]

The pure trans isomers of both dopants induced a right-handed helix in all three nematic hosts. In the next step, we investigated the effect of trans-to-cis isomerization of the dopants on the induced pitch values and helix handedness. Photoinduced variations in HTP values and the pitch were directly observed as a change in distance between the Cano lines when the sample in a wedge cell was observed with a polarized optical microscope under UV ($\lambda_{max} = 360$ nm) or visible-light ($\lambda_{max} = 440$ nm) irradiation. During the process of UV irradiation of a CLC mixture containing 1 wt % (*R*)-**1** in E7, we found the distance between the lines to increase considerably and reach a PSS$_{UV}$ state within 90 s. This occurred because of the elongation of the helical pitch arising from the decrease in HTP of the dopant due to trans−cis isomerization. We calculated a change of ~83% in β of the dopant in going from its initial state to the PSS$_{UV}$ state. Irradiation with 440 nm light reversed the pitch toward the initial state, resulting in an effective 75% change in pitch between the PSS$_{UV}$- and PSS$_{vis}$-induced cholesteric phases. Encouraged by the high HTP of (*R*)-**1** and its good phototunability in E7, we decided to tune the reflection colors in the visible region. LC mixtures containing ~10 wt % (*R*)-**1** showed a blue-colored reflection ($\lambda_{max} = 450$ nm), which upon UV irradiation quickly shifted to the NIR through green- and red-colored reflection bands (Figure 4). The reflection band returned to the initial state after 440 nm irradiation for 90 s.

Light-Controlled Helical Inversion. Cano lines observed for LC mixtures containing 1 wt % (*R*)-**1** in K15 or ZLI-1132 host moved outward and disappeared during UV irradiation and then appeared again upon continued irradiation. We observed a nematic phase (infinite-pitch CLC) in the wedge cell as a result of destabilization of the initially induced cholesteric phase prior to the regeneration of the cholesteric helix (Figure S3 in the Supporting Information). This indeed is an indication of the inversion of the cholesteric handedness.[18,19] Helix inversion occurs when the helix of one handedness unwinds, becomes zero at a certain point, and then forms a helix of the opposite handedness. We observed the inversion of the cholesteric handedness inside wedge cells by the color shift method.[18] While trans-to-cis photoisomerization of (*R*)-**1** in K15 resulted in a cholesteric phase with longer pitch, the pitch length at PSS$_{UV}$ for (*R*)-**1** in ZLI-1132 was found to be shorter. Photoisomerization of (*R*)-**2** in all three NLC hosts passed through a transient nematic phase before stabilizing at the PSS$_{UV}$-induced cholesteric phase. Interestingly, in all of these cases, the switching process was found to be quickly reversible (also through a transient N phase) by 440 nm irradiation. It should be mentioned here that the PSS$_{UV}$-induced cholesteric pitch also returned to the initial state in about 8 h by thermal cis-to-trans isomerization of the dopant molecules in the dark. In comparison with the structurally similar known analogue with ortho substitution,[20] the ability of the chiral dopants (*R*)-**1** and (*R*)-**2** to induce a helical superstructure of opposite handedness might result from the different intermolecular interaction between the dopants and the host upon light irradiation. It is worth noting here that a helical inversion does not necessarily require a change in the overall chiral configuration of the molecule, although it can accompany conformational changes of isomers.[15,19]

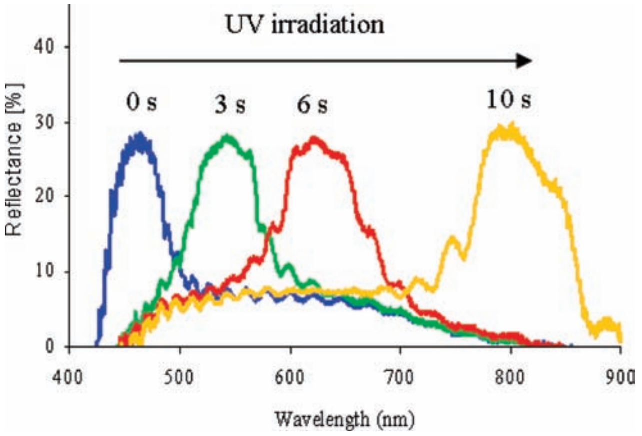

Figure 4. Change in the selective reflection spectra of 10 wt % (*R*)-**1** in achiral liquid crystal host E7 in a 5 μm thick planar cell upon 365 nm UV irradiation at room temperature.

Next, we studied the photoinduced N* → N → N* transitions (and the reverse process by 440 nm light irradiation) for different LC mixtures under planar and homeotropic alignment conditions using a polarized optical microscope. For example, a typical oily streak texture observed for the N* phase of an LC mixture containing 10 wt % (*R*)-**1** in ZLI-1132 under planar alignment conditions was quickly transformed into a planar N texture upon irradiation with UV light (Figure 5a,b). As the sample in the N phase was rotated between fixed crossed polarizers, an extinguishing orientation of the cell was found when the orientation of the molecular director was along one of the polarizer directions (Figure 5c). This transient N phase was quickly transformed into an N* phase upon continued UV irradiation for a few more seconds (Figure 5d). The whole switching process was reversible with 440 nm irradiation.

Determination of Helical Inversion in Long-Pitch Cholesteric Phase. In order to directly measure the opposite helicity in PSS$_{UV}$- and PSS$_{vis}$-induced CLC films, we developed a new

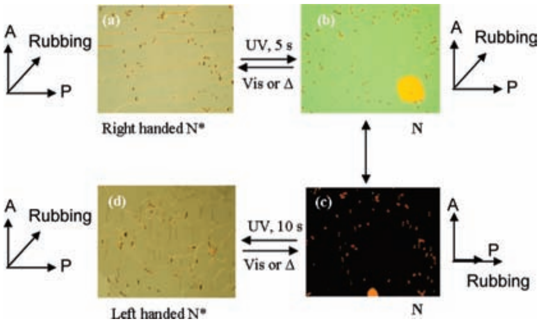

Figure 5. Polarized optical photomicrographs of a planar aligned N* film containing 10 wt % (*R*)-**1** in ZLI-1132 at room temperature, showing reversible phase transitions occurring by light irradiation of the sample inside a 5 μm cell: (a) oily streak texture of the N* phase before irradiation; (b) N phase obtained by exposure of the sample to UV irradiation; (c) extinguishing orientation of the N cell by rotation between crossed polarizers; (d) regeneration of the oily streak texture of the N* phase upon continued irradiation.

method that allowed us to determine the handedness of long-pitched cholesterics.[25] We used a slab cell whose inner surfaces had been coated with an alignment layer of PI-2555 and rubbed antiparallel in order to get a homogeneous alignment. The cell gap was measured by the interference method using a USB4000 spectrometer prior to the filling with LC. The cell was then filled with the cholesteric LC mixture [1.5 wt % (*R*)-**2** in achiral LC host E7]. The cell was then placed under a polarizing microscope, and the transmittance versus wavelength data were recorded. Inside the cell, the cholesteric LC twists at a constant rate in order to match the boundary conditions. For such a geometry, the transmittance, T, can be calculated as follows:

$$T = \cos^2(\alpha_p - \alpha_a - \Phi) - \sin^2(\zeta)\sin[2(\alpha_p - \Phi)]\sin(2\alpha_a) - \frac{\Phi^2}{\zeta^2}\sin^2(\zeta)\cos[2(\alpha_p - \Phi)]\cos(2\alpha_a) - \frac{\Phi}{2\zeta}\sin(2\Theta)\sin[2(\alpha_p - \alpha_a - \Phi)] \quad (3)$$

where α_p and α_a represent the angles that the polarizer and the analyzer, respectively, make with the input rubbing direction, Φ is the total twist of the cholesteric LC, and $\Theta = [\Phi^2 + (\pi\Delta nd/\lambda)^2]^{1/2}$.[9a] However, in order to mimic the measured spectrum with the calculated one, we need to know the dependence of the birefringence with wavelength, which can be expressed as follows:

$$\Delta n = G\frac{\lambda^2\lambda*^2}{\lambda^2 - \lambda*^2} \quad (4)$$

where G is a temperature-dependent quantity related to the order parameter and $\lambda*$ is the mean wavelength of the UV absorption band. Both parameters are well-known for E7 and were obtained from the literature. By substituting eq 4 into eq 3, we can match the measured spectrum with the calculated one. Transmittance as a function of wavelength was measured when the polarizer angle and the rubbing direction were parallel ($\alpha_p = 0$), and the analyzer made an angle of $\alpha_a = 20°$ with respect to the polarizer. Since the cell was rubbed antiparallel, the total twist Φ must be a multiple of π and can be calculated when the chiral dopant concentration, HTP, and thickness d are known. The only unknown parameter for using this equation to fit the measured data is the handedness signal (+ for right-handed or − for left-handed), which we used as a fitting parameter. Since we already measured the HTP of dopants in their initial and photoisomerized states, it was easy to predict that in a 4.9 μm cell, the right-handed conformation would have 5π turns [HTP = +32 for a mixture of E7 and 1.5 wt % (*R*)-**2**] while the left-handed conformation would have −2π turns (HTP = −10) to match the boundary conditions. The measured and simulated data are shown in Figure 6. The small oscillation seen in the measured data is due to the LC−substrate interface. Figure 6a corresponds to the right-handed cholesteric sample obtained before any UV light irradiation by using various input parameters and the number of turns as equal to 5π. Figure 6b corresponds to the PSS_{UV}-induced left-handed cholesteric phase after 365 nm irradiation having the same input parameters as used for the right-handed cholesteric phase except for the number of turns, which we had taken as −2π. As we can see, the agreement between the measured data and the simulated data is very good and matches well with the known values of the cell gap and HTP. Irradiation of the PSS_{UV}-induced cholesteric phase with visible light switched it back to the initial state with a right-handed helicity. Thus, we unambiguously proved the switching of cholesteric handedness by UV and visible-light irradiation.

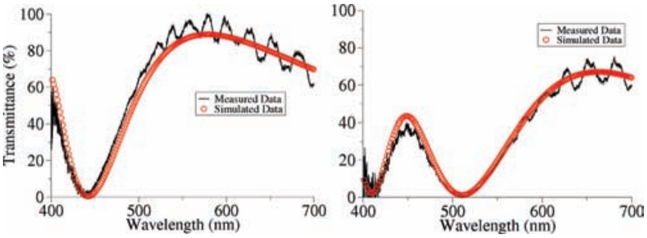

Figure 6. Transmittance vs wavelength for 1.5 wt % (*R*)-**2** in achiral LC host E7: (left) initial right-handed cholesteric phase; (right) left-handed cholesteric phase after irradiation at 365 nm. The black lines represent the measured data, while the red lines represent the simulated data, for which the parameters of the cell were input parameters and the handedness signal was the fitting parameter. The agreement is very good and mimics the cell gap and HTP measured a priori.

The magnitude of the HTP of a particular dopant in a given NLC host is a characteristic property of the chiral dopant and its ordering in the LC matrix. In binaphthyl derivatives, the chirality results from the hindered torsional rotation about the 1,1′-C−C bond between the two naphthyl moieties. A number of conformers are expected for the present chiral dopants, corresponding to different values of the dihedral angles. Therefore, we attribute the difference in HTP and the helical twist inversion upon light irradiation to these conformational changes. In the structures derived from energy minimization calculations, we found that a transoid form of the dopant is thermally more stable and induces a right-handed helix while a cisoid form obtained after UV irradiation induces a left-handed helix.

Conclusions

Two cyclic azobenzenophanes with axial chirality employed as phototunable chiral dopants were found to be able to induce helical superstructure in three structurally different achiral LC hosts and reversibly control the selective reflection colors from blue to NIR. More importantly, the different switching states of the light-driven chiral cyclic dopants (i.e., trans−cis isomerization) were capable of inducing a helical handedness inversion in the induced self-organized helical superstructures. Therefore,

---

(25) Hurley, S. Liquid Crystal Displays for Pixelated Glare Shielding Eyewear. Ph.D. Dissertation, Kent State University, Kent, OH, 2010.

we could obtain a rapid change in the sign of the helical handedness by alternating UV and visible-light irradiation. Fast switching (a few seconds) of the handedness combined with tunability of the reflection colors over the entire visible range by light irradiation opens new perspectives for future applications. Furthermore, a new method was developed to allow us to directly determine the handedness of the long-pitched self-organized helical cholesteric phase.

Acknowledgment. This work was supported by the Air Force Office of Scientific Research (FA9550-09-1-0193), the Materials and Manufacturing Directorate of the Air Force Research Laboratory, and the National Science Foundation (IIP 0750379).

Supporting Information Available: Experimental details, methods, syntheses, textures, and pitch change observed by light irradiation. This material is available free of charge via the Internet at http://pubs.acs.org.

JA108437N